

Green Oxidative Degradation of Methyl Orange with Copper(II) Schiff Base Complexes as Photo-Fenton-Like Catalysts

Bao-Li Fei,^{*[a,b]} Qing-Ling Yan,^[a] Jiang-Hong Wang,^[a] Qing-Bo Liu,^[c] Jian-Ying Long,^[c] Yang-Guang Li,^[d] Kui-Zhan Shao,^[d] Zhong-Min Su,^{*[d]} and Wei-Yin Sun^{*[b]}

Keywords: Schiff bases; Copper; L Methyl orange; Photocatalytic degradation; Fenton-like reaction

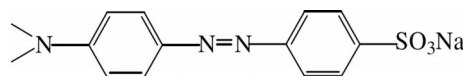
Abstract. Two copper(II) complexes, namely [Cu(HL)Cl] (**1**) and [Cu(HL)Br] (**2**), where HL is the multidentate Schiff base *N*-[(2-oxy-acetate)-benzyl]-2-aminethanol, were synthesized and fully characterized. The Cu^{II} ions in **1** and **2** are pentacoordinate and the coordination arrangement is best described as distorted square-pyramidal. The degradation

of methyl orange (MO) was investigated using **1** and **2** as homogeneous photo-Fenton-like catalysts. **1** and **2** exhibited similar catalytic activity at neutral pH. The results suggest that they have advantages on catalyzing efficient degradation of organic dye through photo-Fenton-like reaction.

Introduction

Azo dyes represent an important class of environmental water contaminations due to their toxicity and slow degradation.^[1] To avoid the dangerous accumulation of such dyes in environment, it is urgent to develop effective methods to degrade this type of pollutant to less harmful compounds or more desirable mineralization products. Methyl orange (MO, Scheme 1) is a widely used sulfonated azo dye and is often chosen as pollution model in water treatment industry. Intense work has been undertaken for degradation of MO into harmless products. Non-destructive technological processes, such as traditional physical and chemical techniques are not suitable for the degradation of MO.^[2] Although biological treatment methods for the degradation of MO has appeared in literature,^[3,4] the environmentally-friendly advanced oxidation processes (AOPs) based on the in situ generation of hydroxyl radical ([•]OH), which degrades most organic pollutants quickly and non-selectively, have been explored to act as alternatives to the conventional and biological treatment methods. It is reported

that AOPs are effective techniques to degrade a wide range of azo dyes.^[1] Fenton reaction (Fe²⁺ or Fe³⁺/H₂O₂) and Photo-Fenton reaction (H₂O₂/Fe²⁺ or Fe³⁺/UV) are regarded as two of the most promising AOPs for the treatment of dye contaminated water, due to advantages such as safety, simplicity, cleanliness and energy conservation without causing secondary pollution.^[5,6] The incorporation of UV radiation into the Fenton process causes a dramatic increase in the [•]OH formation efficiency.^[7] Such processes have the ability to completely decolorize and partially mineralize dyes in short reaction time.^[7]



Scheme 1. Structural formula of methyl orange (MO).

The Fe^{II} based Fenton reaction and its modifications have been used for removing various pollutants.^[8] However, Fenton's reagent can work only in a narrow acidic pH range (pH 2–4) and are not able to completely decompose some dyes; these drawbacks limited its wider application.^[9] Consequently, to develop novel Fenton-like reagent with higher and practical activity is a challenging issue. Few research groups have transferred their attention to the investigations on the similar reactions based on Cu^{II}, because copper-based radicals generating systems have been used for the degradation of lignin.^[10] Cu^{II} can replace Fe^{II} for similar uses in a wider pH (3–9) range and a broad substrate specificity.^[11] After copper ion is coordinated with pyridine, organic acids, amino acids, and other chelating agents in water solutions, its catalytic activity as Fenton-like reagent will be dramatically enhanced.^[8,9,11–13] Masarwa et al. pointed out that copper(II) complex/H₂O₂ system in aqueous solution could be considered as Fenton-like reagent.^[14] Copper(II) complexes can activate H₂O₂ to produce active oxygen species, but the exact active oxygen species and their catalytic mechanisms were not confirmed yet.^[14] Furthermore, the

* Dr. B.-L. Fei, Prof. Dr. Z.-M. Su, Prof. Dr. W.-Y. Sun
Fax: +86-258-541-8873
E-Mail: hgfb1@njfu.edu.cn

[a] College of Chemical Engineering
Nanjing Forestry University
Nanjing 210037, P. R. China

[b] Coordination Chemistry Institute
State Key Laboratory of Coordination Chemistry
Nanjing University
Nanjing 210093, P. R. China

[c] College of Science
Nanjing Forestry University
Nanjing 210037, P. R. China

[d] Institute Functional Material Chemistry
Faculty of Chemistry
Northeast Normal University
Changchun 130024, P. R. China

Supporting information for this article is available on the WWW under <http://dx.doi.org/10.1002/zaac.201300562> or from the author.

structures of the most documented catalysts are usually not very distinct, which makes the structure-activity relationship remain unclear. *Barb* and *Kadiiska* proposed that a series of radical species including $\cdot\text{OH}$ and HO_2/O_2^- were involved in this kind of catalysis.^[14] Therefore, it is necessary to clarify these cloudy points about copper(II) complex based Fenton-like system.

Singh et al. reported that iron(II) Schiff base complex $[\text{Fe}^{\text{II}}\text{-salen}]\text{Cl}$ can be used for photo-remediation of pollutants (dye),^[8] but whether copper(II) Schiff base complex can take the similar function is still unrealized. If it can, what kinds of reactive species should take the responsibility to degrade dyes? Whether the crystal structure has a close relationship with the catalytic ability? To the best of our knowledge, no literature answers these questions especially the second one. So, it is important to use well defined complexes with some similarities in Fenton related reaction, the results of such investigation will provide useful clue to design new efficient Fenton-like reagent.

In this work, application of copper(II) Schiff base complexes as photo-Fenton-like catalysts for the degradation of persistent organic dye MO is reported. It is the first time that simple copper(II) Schiff base complexes with similar crystal structure were used as catalysts for the photo-remediation of dye polluted water. It is meaningful that the copper(II) Schiff base complexes utilized in this work show significant Fenton-like reagent performance. This model system may be applicable to the effective treatment of organic pollutants in wastewater.

Results and Discussion

Description of the Structures

The complexes $[\text{Cu}(\text{HL})\text{Cl}]$ (**1**) and $[\text{Cu}(\text{HL})\text{Br}]$ (**2**) [$\text{L} = N$ -[(2-oxy-acetate)benzyl]-2-aminethanol] crystallized in the monoclinic space group $P2_1/n$, with $Z = 4$ and $Z = 3$, respectively. Structural analysis reveals that **1** and **2** consist of chemically similar but crystallographically independent two $[\text{Cu}(\text{HL})\text{X}]$ units ($X = \text{Cl}$ for **1**, Br for **2**). The crystal structures of **1** and **2** with the atomic numbering scheme are shown in Figure 1.

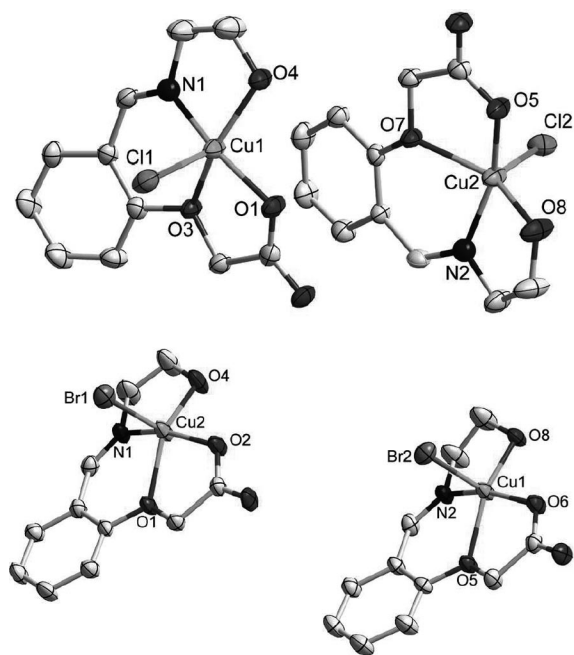


Figure 1. ORTEP views of the molecular structures of **1** (above) and **2** (below) with ellipsoids drawn at the 30% probability level. Hydrogen atoms are omitted for clarity.

It can be seen that the copper(II) ion of each $[\text{Cu}(\text{HL})\text{X}]$ unit is five-coordinate by one imine nitrogen atom, one halide ion, and three other oxygen atoms from hydroxyl, phenolic hydroxyl, and carboxylate, respectively. Selected bond lengths and angles are listed in Table 1 and Table 2.

As displayed in Figure 1, in the $[\text{Cu1}(\text{HL})\text{Cl1}]$ unit of **1**, N1, O1, O3, and O4 bind at the basal plane, and the axial coordination site of the central copper atom is occupied by Cl1. The angles observed between the axial and equatorial atoms O1–Cu1–Cl1, N1–Cu1–Cl1, O4–Cu1–Cl1, and O3–Cu1–Cl1 are $99.09(11)^\circ$, $99.68(13)^\circ$, $113.25(12)^\circ$, and $97.29(9)^\circ$, respectively. The equatorial Cu–N and Cu–O distances Cu1–N1, Cu1–O1, Cu1–O3, and Cu1–O4 are $1.909(4)$ Å, $1.904(3)$ Å, $2.104(3)$ Å, and $1.993(3)$ Å, respectively. The axial Cu1–Cl1 distance [$2.3632(16)$ Å] is longer than any bond length in the basal plane. The corresponding Cu–N and Cu–O distances in

Table 1. Selected bond lengths /Å and bond angles /° for complex **1**.

Cu1–N1	1.909(4)	Cu1–O1	1.904(3)	Cu1–O3	2.104(3)
Cu1–O4	1.993(3)	Cu1–Cl1	2.3632(16)		
Cu2–O5	1.912(3)	Cu2–N2	1.923(4)	Cu2–O8	1.999(4)
Cu2–O7	2.135(3)	Cu2–Cl2	2.3140(16)		
O1–Cu1–N1	159.78(17)	O1–Cu1–O4	97.10(14)	N1–Cu1–O4	82.32(15)
O1–Cu1–O3	81.16(12)	N1–Cu1–O3	89.05(14)	O4–Cu1–O3	149.22(14)
O1–Cu1–Cl1	99.09(11)	N1–Cu1–Cl1	99.68(13)	O4–Cu1–Cl1	113.25(12)
O3–Cu1–Cl1	97.29(9)				
O5–Cu2–N2	157.03(16)	O5–Cu2–O8	95.93(15)	N2–Cu2–O8	81.52(16)
O5–Cu2–O7	80.34(12)	N2–Cu2–O7	88.42(13)	O8–Cu2–O7	144.16(16)
O5–Cu2–Cl2	101.97(12)	N2–Cu2–Cl2	99.33(12)	O8–Cu2–Cl2	117.82(15)
O7–Cu2–Cl2	97.68(9)				

Table 2. Selected bond lengths /Å and bond angles /° for complex **2**.

Cu1–O6	1.901(3)	Cu1–N2	1.919(4)	Cu1–O8	1.994(3)
Cu1–O5	2.080(3)	Cu1–Br2	2.5417(10)		
Cu2–O2	1.907(3)	Cu2–N1	1.926(4)	Cu2–O4	1.998(4)
Cu2–O1	2.102(3)	Cu2–Br1	2.4869(11)		
O6–Cu1–N2	161.63(18)	O6–Cu1–O8	98.34(16)	N2–Cu1–O8	82.74(16)
O6–Cu1–O5	81.94(13)	N2–Cu1–O5	89.62(15)	O8–Cu1–O5	155.74(15)
O6–Cu1–Br2	97.99(12)	N2–Cu1–Br2	99.15(14)	O8–Cu1–Br2	107.59(11)
O5–Cu1–Br2	96.32(10)				
O2–Cu2–N1	159.4(2)	O2–Cu2–O4	96.17(15)	N1–Cu2–O4	81.94(17)
O2–Cu2–O1	81.09(13)	N1–Cu2–O1	89.44(15)	O4–Cu2–O1	147.21(17)
O2–Cu2–Br1	101.58(14)	N1–Cu2–Br1	97.79(14)	O4–Cu2–Br1	114.95(14)
O1–Cu2–Br1	97.50(10)				

the [Cu2(HL)Cl2] unit of **1** are longer than that of the [Cu1(HL)Cl1] unit, however, the Cu–Cl distance is in the reverse order. Each central copper(II) atom of **1** displays a distorted square pyramidal (SPY) arrangement with values of the structural distortion parameter τ of 0.17 and 0.21 for Cu1 and Cu2, respectively. The structural distortion parameter is defined as $\tau = (\beta - a)/60^\circ$, where a and β are the two largest ligand–metal–ligand angles. It is a useful geometrical discrimination, $\tau = 1$ for idealized trigonal bipyramidal (TBPY) ($a = 120^\circ$ and $\beta = 180^\circ$) and $\tau = 0$ for idealized SPY arrangement ($a = \beta = 180^\circ$).^[15]

The crystal unit of **2** is similar to that of **1** (Figure 1). In the case of Cu1, the square plane is defined by the N2, O5, O26, and O8, and Br2 occupies the apical position. The angles observed between the axial and equatorial atoms O6–Cu1–Br2, N2–Cu1–Br2, O8–Cu1–Br2, and O5–Cu1–Br2 are 97.99(12)°, 99.15(14)°, 107.59(11)° and 96.33(10)°, respectively. The τ values for the crystallographically independent Cu1 and Cu2 of complex **2** are 0.10 and 0.20, respectively, indicating the coordination arrangement of each central copper(II) atom is distorted square pyramidal. By comparison, Cu–N and Cu–O distances in the [Cu2(HL)Br1] unit of **2** are longer than that of the [Cu1(HL)Br2] unit, and the apical Cu–Br bond lengths are 2.5417(10) Å for Cu1 and 2.4869(11) Å for Cu2.

The τ data of **1** and **2** indicate that the copper(II) ions in the crystal structures of **1** and **2** have similar coordination arrangements. The bond lengths of Cu–Cl are shorter than that of Cu–Br, similar result has appeared in the literature.^[15]

Photo-Fenton Catalytic Activity for the Degradation of MO

MO was selected as model dye to evaluate the photo-Fenton-like catalytic behaviors of **1** and **2**, due to its environmental significance and non-biodegradation. The effect of each reaction conditions, such as concentration of catalyst **1**, H₂O₂, and MO and pH was studied to optimize the degradation conditions (Figures S1–S4 in the Supporting Information). The photoreaction was carried out by changing one of the parameters and keeping the others fixed. Because the two complexes have similar structures and catalytic activities only the results of complex **1** are discussed in detail herein.

Kinetics of MO Degradation

The changes of MO concentration as a function of reaction time under different conditions are illustrated in Figure 2. It is observed that MO degraded slowly under UV light illumination, whereas the reaction rate was evidently enhanced in the presence of H₂O₂ alone or catalyst (**1/2**) combined with H₂O₂. A comparison of the different processes leads us to conclude that the involvement of the photo-Fenton-like catalyst **1/2** sharply improved the degradation efficiency, and **1** and **2** exhibited similar activity under the same concentration. The reason that **1** and **2** displayed similar catalytic activity is owing to their similar molecular structure, and the slight difference in photocatalytic activity is caused by the different coordination anion radius, which has an effect on the generation rate of the intermediate product [Cu⁺O₂H(HL)X] ($X = \text{Cl}$ for **1**, Br for **2**) (see Supporting Information: proposed reaction pathways Section).

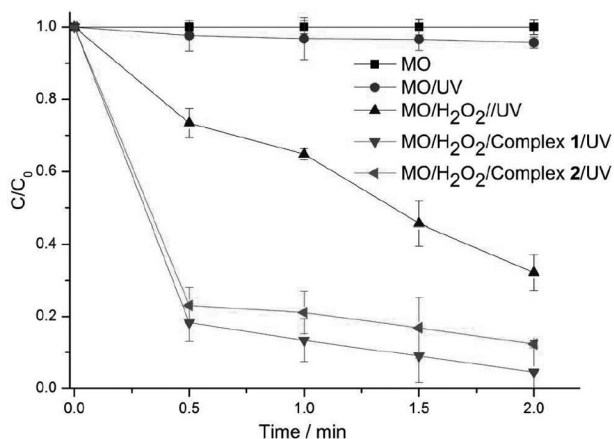


Figure 2. Degradation kinetics of MO in different reaction systems. Experimental conditions: MO, 2×10^{-5} M; H₂O₂, 2.40×10^{-2} M; **1/2**, 3.11×10^{-6} M; pH = 6.50 for **1**; pH = 6.70 for **2**. UV light, 300 W.

The degradation of MO in the absence of any external oxidizing agent was caused by hydroxyl radicals $\cdot\text{OH}$ produced by UV photolysis of water [Equation (1)],^[16] while in the presence of H₂O₂, hydroxyl radicals $\cdot\text{OH}$ were generated by UV photolysis of H₂O₂ [Equation (2)].^[17] Hence, the reaction rate was dramatically increased when H₂O₂ was added to the dye

solution.^[17] The $\cdot\text{OH}$ radical can destroy the dye to generate intermediate or mineralization products.^[18]



In the case of photo-Fenton-like systems, according to Sawyer and others,^[19–21] the Fenton-like catalysts (**1/2**) enhanced the reaction rate through activating H_2O_2 to generate the intermediate product $[\text{Cu}^+\text{O}_2\text{H}(\text{HL})\text{X}]$ ($\text{X} = \text{Cl}$ for **1**, Br for **2**), which could react with another H_2O_2 molecule to give $\cdot\text{OH}$ (see Supporting Information: proposed reaction pathways Section).

UV/Vis Spectra of MO during the Photo-Fenton-like Process

The temporal evolution of the spectral changes of MO for MO/UV/ H_2O_2 /**1** system is displayed in Figure 3. In general, the UV/Vis spectra of MO solution showed two characteristic absorption peaks at 272 and 465 nm. The UV band at 272 nm was ascribed to the $\pi \rightarrow \pi^*$ transition of the aromatic rings in the MO molecule, whereas the band in the visible region (465 nm) was attributed to the conjugated structure formed by the azo bond under the strong influence of the electron-donating dimethylamino group.^[22] The rate of degradation was recorded with respect to the changes in intensity of absorption peak at 465 nm.

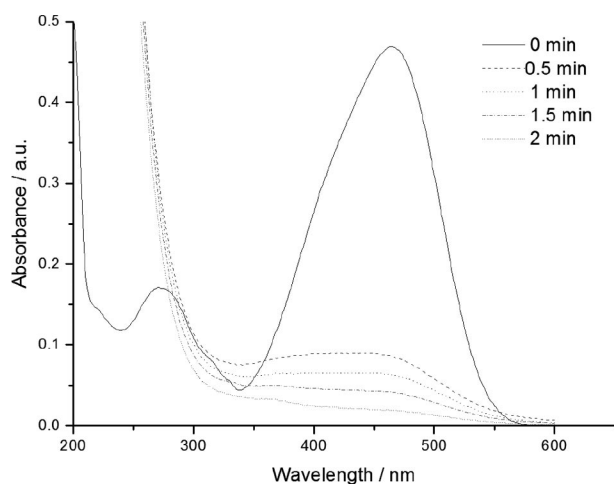


Figure 3. Changes in the absorption spectrum with time observed for the homogeneous photo-Fenton-like process catalyzed by **1**. Experimental conditions: MO, 2×10^{-5} M; H_2O_2 , 2.40×10^{-2} M; **1**, 3.11×10^{-6} M; pH = 6.50. UV light, 300 W.

In the presented study, the maximum absorption band of MO in the visible region decreased dramatically to about zero in 2 min with no new absorption band appearing in the visible region. This indicates that the decolorization of the MO was rather complete. In addition, the absorption peak at 272 nm developed quickly and diminished all over the spectral window and no more specific peak can be detected under the current experimental condition. The disappearance of the absorption peaks corresponding to MO indicates that MO was degraded.

Effect of Scavenger on Oxidizing Species

It is generally accepted that $\cdot\text{OH}$ radicals is the main oxidizing species in the oxidation of azo dye by photo-Fenton-like reaction. To detect whether other reactive species such as free superoxide (HO_2/O_2^-) and singlet oxygen ($^1\text{O}_2$) also took some responsibility for the degradation of MO, the photolysis was conducted in the presence of a series of added scavengers, NaBr, effective scavengers for $\cdot\text{OH}$ radicals,^[23] benzoquinone, an effective scavenger for HO_2/O_2^- radicals,^[24] and NaN_3 , an effective scavenger for $^1\text{O}_2$ in separate experiments,^[25] while the other conditions were identical. Although this method is not absolutely accurate in detecting the oxidizing species, it at least told us what species were possibly involved in the current reaction.

Figure 4 shows that all the scavengers suppressed the photo-degradation rate to some degree. A fact that bromide and azide ions could coordinate with central copper atoms to compete with H_2O_2 and thus retarded the reaction rate to some degree should be considered. Notably, benzoquinone was reported to have photochemical reactivity, but it really obstructed the reaction speed in this case. In addition, NaBr and NaN_3 showed different suppressing ability means they mainly acted as scavengers. Based on the above mentioned points, the experimental results shown here leads us to conclude that $^1\text{O}_2$, $\cdot\text{OH}$, and HO_2/O_2^- radicals should all take part in the degradation, but which one is the most important could not be determined at the moment.

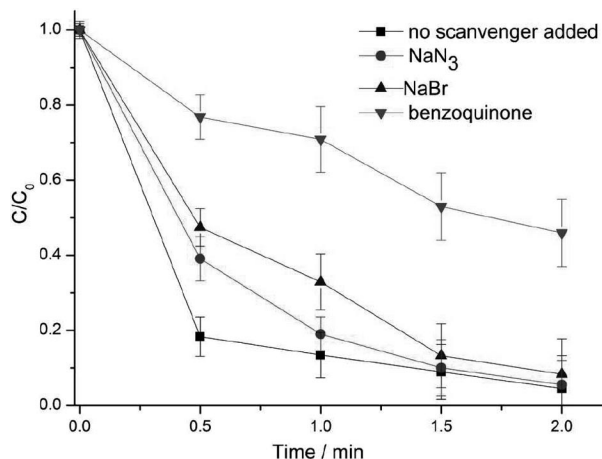


Figure 4. Degradation kinetics of the photo-Fenton-like reactions. Experimental conditions: MO, 2×10^{-5} M; H_2O_2 , 2.40×10^{-2} M; **1**, 3.11×10^{-6} M; NaBr, 0.1 M; benzoquinone, 0.1 M; NaN_3 , 4.3×10^{-4} M; pH = 6.50. UV light, 300 W.

Mineralization Studies

Complete decolorization of MO does not necessary mean that it was completely oxidized into CO_2 and H_2O , that is mineralization, as reactive intermediates containing benzene rings can be formed during oxidation. Therefore, it is important to evaluate the mineralization of organic dye. The mineralization degree of MO was evaluated by monitoring the change in the total organic carbon (TOC), as shown in Figure 5. The TOC

analysis provides information on whether or not MO molecules are completely converted into CO_2 and H_2O . TOC_0 referred to the TOC content of the initial MO solution and TOC_t referred to the TOC content of the reaction solution at reaction time t . Under the optimal conditions, about 73% (**1**) and 84% (**2**) mineralization in 10 min was obtained. The removal of TOC achieved confirmed that the photodegradation of MO was accompanied by partial mineralization and the decolorization rate was much faster than mineralization rate. Such high TOC removal rate indicates that some benzene substituted intermediates and some ring-open up degradation products of benzene such as formic acid, acetic acid maybe both present in the final solution.^[26,27] Anyway, the results demonstrate that **1** and **2** have some advantage on photocatalytic degradation of dye pollutants.

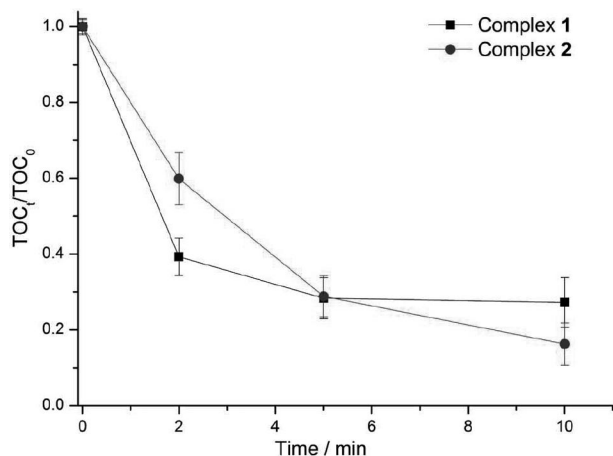


Figure 5. TOC change of the photo-Fenton-like reactions. Experimental conditions: MO, 2×10^{-5} M; H_2O_2 , 2.40×10^{-2} M; **1/2**, 3.11×10^{-6} M; pH = 6.50. UV light, 300 W.

Conclusions

Photodegradation of MO was studied using **1** or **2** as homogeneous photo-Fenton-like catalyst. The results show that **1** and **2** were excellent photo-Fenton's catalysts and the property was significantly affected by the initial pH and the concentration of hydrogen peroxide and MO. In addition, the photocatalytic property of this type of complex has some relationship with structure; the coordination anion of the catalyst can affect the photocatalytic activity in some degree by tuning the steric hindrance during the process of the formation of the intermediate product. The photo-Fenton-like reactions were carried out without the acidification process, this is an important advantage because it is well-known that one major drawback of homogeneous Fenton process is the narrow acidic pH range, which is unfavorable in practice due to the costs of acidification during processing and neutralization after treatment. It was very likely that active oxidizing species $\cdot\text{OH}$, HO_2/O_2^- , and 1O_2 were involved in the photo-Fenton-like reaction. The photo-Fenton-like processes in this work not only led to complete decolorization of MO in relatively short time (about 5 min) but also partially mineralized the azo dye. These experi-

mental results not only are encouraging but also present a new clue to develop practical highly active photo-Fenton-like catalysts using under neutral pH condition.

Experimental Section

Materials: All chemicals were commercial available and used without further purification unless otherwise noted. *o*-Oxy-acetatebenzaldehyde was prepared according to literature and characterized by IR, ^1H NMR, MS, and C, H, N analysis.^[28]

Synthesis of [Cu(HL)Cl] (1**):** An absolute methanol solution (5 mL) of *o*-oxy-acetatebenzaldehyde (0.0180 g, 1 mmol) was added dropwise to a vigorously stirred solution of ethanolamine (0.062 g, 1 mmol) in absolute methanol (5 mL) under reflux. The resulting yellow solution was heated to reflux for 6 h before cooling to room temperature. To this yellow H_2L solution, a solution of copper(II) chloride (0.172 g, 1 mmol) in methanol (5 mL) was added slowly under vigorously stirring. The resulting solution was stirred for 1 h at 30 °C. Green block single crystals suitable for X-ray analysis were obtained on slow diffusion of diethyl ether into the solution after one week. Yield: 15% (0.096 g). IR (KBr): $\tilde{\nu} = 3424$ (br), 1654 (s), 1605 (s), 1400 (m), 1290 (w), 1222 (m) cm^{-1} . $\text{C}_{22}\text{H}_{24}\text{Cl}_2\text{Cu}_2\text{N}_2\text{O}_8$ (642.41 $\text{g}\cdot\text{mol}^{-1}$): calcd. C 41.13; H 3.77; N 4.36%; found C 41.27; H 3.74; N 4.21%.

Synthesis of [Cu(HL)Br] (2**):** The copper(II) complex **2** was prepared by following a similar procedure as described above using copper(II) bromide (0.226 g, 1 mmol) in methanol (5 mL) and acetonitrile (2:1, V/V) mixture instead of copper(II) chloride. Yield: 11% (0.107 g). IR (KBr): $\tilde{\nu} = 3436$ (br), 1655 (s), 1605 (s), 1400 (m), 1290 (w), 1221 (m) cm^{-1} . $\text{C}_{11}\text{H}_{12}\text{BrCuNO}_4$ (365.67 $\text{g}\cdot\text{mol}^{-1}$): calcd. C 36.09; H 3.28; N 3.83%; found C 36.17; H 3.37; N 3.81%.

X-ray Crystallography: The data was recorded with a Bruker ApexII CCD diffractometer with graphite-monochromated $\text{Mo-K}\alpha$ radiation ($\lambda = 0.71069$ Å for **1**, and 0.71073 Å for **2**) at 293 K. Empirical absorption correction was applied. The structure of **1** was solved by direct methods of SHELXS-97 and refined by full-matrix least-squares techniques using the SHELXL-97 program. All the non-hydrogen atoms were refined anisotropically.

Crystallographic data (excluding structure factors) for the structures in this paper have been deposited with the Cambridge Crystallographic Data Centre, CCDC, 12 Union Road, Cambridge CB21EZ, UK. Copies of the data can be obtained free of charge on quoting the depository numbers CCDC-933249 (for **1**) and CCDC-933248 (for **2**) (Fax: +44-1223-336-033; E-Mail: deposit@ccdc.cam.ac.uk, <http://www.ccdc.cam.ac.uk>). Details of the crystallographic data and structure refinement parameters for compounds **1** and **2** are as follows:

Crystal Data for 1: $\text{C}_{22}\text{H}_{24}\text{Cl}_2\text{Cu}_2\text{N}_2\text{O}_8$, $M = 642.41$, monoclinic, space group $P2_1/n$, $a = 9.7000(12)$ Å, $b = 17.983(2)$ Å, $c = 14.7200(18)$ Å, $\beta = 104.154(2)^\circ$, $V = 2489.7(5)$ Å³, $Z = 4$, $F(000) = 1034$, $\rho_{\text{calcd}} = 1.714$ g/cm^3 , $\mu = 1.973$ mm^{-1} , min/max transmission = 0.6279/0.6707, $\theta_{\text{max}} = 25.00^\circ$, measured reflections = 12267, unique reflections = 4388, $R_1 = 0.0440$, $wR_2 = 0.0994$ for 2775 reflections with $I > 2\sigma(I)$. The goodness-of-fit on F^2 was equal to 1.000.

Crystal Data for 2: $\text{C}_{11}\text{H}_{12}\text{BrCuNO}_4$, $M = 365.67$, monoclinic; space group $P2_1/n$, $a = 9.8276(12)$ Å, $b = 18.292(2)$ Å, $c = 14.7427(18)$ Å, $\beta = 103.187(2)^\circ$, $V = 2580.3(6)$ Å³, $Z = 8$, $F(000) = 1448$, $\rho_{\text{calcd}} = 1.883$ g/cm^3 , $\mu = 4.794$ mm^{-1} , min/max transmission = 0.4326/0.5534, $\theta_{\text{max}} = 26.04^\circ$, measured reflections = 14535, unique reflections =

5494, $R_1 = 0.0422$, $wR_2 = 0.0867$ for 2803 reflections with $I > 2\sigma(I)$. The goodness-of-fit on F^2 was equal to 0.987.

Photoreactor and Light Source: The reactor used in all experiments was a XPA-VII type photochemical apparatus (Xujiang Machine Factory, Nanjing, China). A 300 W high pressure mercury lamp equipped with cool water circulating filter to absorb the near IR radiation was used as the UV light source. The lamp was always allowed to stabilize before use.

Evaluation of Photocatalytic Activity: Freshly prepared aqueous solutions of MO (2×10^{-5}) in the presence of **1** (3.11×10^{-6} M) or **2** (3.11×10^{-6} M) and H_2O_2 (2.40×10^{-2} M) were magnetically stirred for 30 min in the dark. Then the solutions were started to photocatalytic degradation under aerated conditions at ambient temperature in the presence/absence of UV light irradiation. The solutions were magnetically stirred throughout the experiment. At given time intervals, 3 mL aliquots were sampled and subsequently analyzed by TU-1901 UV/Vis spectrophotometer (Beijing Purkinje General Instrument Co., Ltd.) to record the temporal UV/Vis spectral variations of the dye. The MO concentration was determined by measuring the maximum absorbance at 465 nm as a function of irradiation time using the UV/Vis spectrophotometer. All the tests were carried out three times to ensure the reproducibility.

Supporting Information (see footnote on the first page of this article): Figure S1: Effect of photo-Fenton-like catalyst concentration on the degradation of MO. Experimental conditions: MO, 2×10^{-5} M; H_2O_2 , 2.40×10^{-2} M; **1**, 1.56 – 6.22×10^{-6} M; pH = 6.50 for **1**. UV light, 300 W. Figure S2: Effect of pH on the degradation of MO. Experimental conditions: MO, 2×10^{-5} M; H_2O_2 , 2.40×10^{-2} M; **1**, 3.11×10^{-6} M. UV light, 300 W; Figure S3: Effect of MO concentration on the degradation. Experimental conditions: H_2O_2 , 2.40×10^{-2} M; pH = 6.50; **1**, 3.11×10^{-6} M. UV light, 300 W; Figure S4: Effect of H_2O_2 concentration on the degradation of MO. Experimental conditions: MO, 2×10^{-5} M; pH = 6.50; **1**, 3.11×10^{-6} M. UV light, 300 W. Proposed reaction pathways.

Acknowledgements

The authors gratefully acknowledge the financial support from State Key Laboratory of Coordination Chemistry of Nanjing University, Nanjing Forestry University and the Priority Academic Program Development of Jiangsu Higher Education Institutions, College and University Graduate Research Innovation Project of Jiangsu Province (No. CXLX13_517), and University Science Research Project of Jiangsu Province (No. 13KJB220006).

References

- [1] R. G. El-sharkawy, A. S. B. El-din, S. E. H. Etaiw, *Spectrochim. Acta A* **2011**, *79*, 1969–1975.
- [2] M. R. Elahifard, M. R. Gholami, *Environ. Prog. Sustain. Energy* **2012**, *31*, 371–378.
- [3] A. M. T. Silva, J. Herney-Ramirez, U. Soylemez, L. M. Madeira, *Appl. Catal. B* **2012**, *121*–122, 10–19.
- [4] M. M. Tauber, G. M. Gubit, A. Rehorek, *Bioresource Technol.* **2008**, *99*, 4213–4220.
- [5] J. Macías-Sánchez, L. Hinojosa-Reyes, J. L. Guzmán-Mar, J. M. Peralta-Hernández, A. Hernández-Ramírez, *Photochem. Photobiol. Sci.* **2011**, *10*, 332–337.
- [6] I. Grčić, D. Vujević, N. Koprivanac, *Chem. Eng. J.* **2010**, *157*, 35–44.
- [7] M. S. Lucas, J. A. Peres, *Dyes Pigm.* **2006**, *71*, 236–244.
- [8] S. Gazi, R. Ananthakrishnan, N. D. P. Singh, *J. Hazard. Mater.* **2010**, *183*, 894–901.
- [9] J. Ran, X. Li, Q. Zhao, Z. Qua, H. Li, Y. Shi, G. Chen, *Inorg. Chem. Commun.* **2010**, *13*, 526–528.
- [10] P. Verma, P. Baldrian, J. Gabriel, T. Trnka, F. Nerud, *Chemosphere* **2004**, *57*, 1207–1211.
- [11] P. Verma, V. Shah, P. Baldrian, J. Gabriel, P. Stopka, T. Trnka, F. Nerud, *Chemosphere* **2004**, *54*, 291–295.
- [12] J. M. L. Martinez, M. F. L. Denis, L. L. Piehl, E. R. de Celis, G. Y. Buldain, V. C. D. Orto, *Appl. Catal. B* **2008**, *82*, 273–283.
- [13] Y. Li, Z. Yi, J. Zhang, M. Wu, W. Liu, P. Duan, *J. Hazard. Mater.* **2009**, *171*, 1172–1174.
- [14] J. M. Li, X. G. Meng, C. W. Hu, J. Du, X. C. Zeng, *J. Mol. Catal. A* **2009**, *299*, 102–107.
- [15] A. W. Addison, T. N. Rao, J. Reedijk, J. Rijn, G. C. Verschoor, *J. Chem. Soc. Dalton Trans.* **1984**, 1349–1356.
- [16] G. A. Bowmaker, C. D. Nicola, C. Pettinari, B. W. Skelton, N. Somers, A. H. White, *Dalton Trans.* **2011**, *40*, 5102–5115.
- [17] S. Haji, B. Benstaali, N. Al-Bastaki, *Chem. Eng. J.* **2011**, *168*, 134–139.
- [18] Y. Xu, *Chemosphere* **2001**, *43*, 1103–1107.
- [19] D. T. Sawyer, A. Sobkowiak, T. Matsushita, *Acc. Chem. Res.* **1996**, *29*, 409–416.
- [20] D. T. Sawyer, *Coord. Chem. Rev.* **1997**, *165*, 297–313.
- [21] L. Qin, Y. Gu, G. Y. Li, S. L. Xiao, G. H. Cui, *Transition Met. Chem.* **2013**, *38*, 407–412.
- [22] T. D. Nguyen, N. H. Phan, M. H. Do, K. T. Ngo, *J. Hazard. Mater.* **2011**, *185*, 653–661.
- [23] I. Arslan-Alaton, J. L. Ferry, *Dyes Pigm.* **2002**, *54*, 25–36.
- [24] J. Cao, B. Luo, H. Lin, S. Chen, *J. Mol. Catal. A* **2011**, *344*, 138–144.
- [25] A. Xu, X. Li, H. Xiong, G. Yin, *Chemosphere* **2011**, *82*, 1190–1195.
- [26] R. Zugle, T. Nyokong, *J. Mol. Catal. A* **2013**, *366*, 247–253.
- [27] X. Lu, H. Ma, Q. Zhang, K. Du, *Res. Chem. Intermed.* **2013**, *39*, 4189–4203.
- [28] D. W. Emmons, *Organic Synthesis*, John Wiley and Sons Inc., New York, **1996**, Vol. 46, pp. 28–29.

Received: November 4, 2013
Published Online: May 8, 2014